Stability analysis of spatiotemporal cnoidal waves in cubic nonlinear media

Victor A. Aleshkevich,[1] Alexey A. Egorov,[1] Yaroslav V. Kartashov,[1,2] Victor A. Vysloukh,[3] and Anna S. Zelenina[1]
[1]*Chair of General Physics, Physics Department, M. V. Lomonosov Moscow State University, 119899, Vorobiovy Gory, Moscow, Russia*
[2]*Institute of Photonic Sciences and Department of Signal Theory and Communications, Universitat Politecnica de Catalunya, 08034 Barcelona, Spain*
[3]*Departamento de Fisica y Matematicas, Universidad de las Americas—Puebla, Santa Catarina Martir, codigo postal 72820, Puebla, Cholula, Mexico*
(Received 14 February 2003; published 20 June 2003)

We analyze numerically the modulational instability of spatiotemporal cnoidal waves of cn, dn, and sn types that are periodic along a single space coordinate and are uniform in time. The band of possible increments is calculated for all three types of cnoidal waves as a function of parameter describing the degree of localization of the wave field energy. It is shown that this band transforms into a set of discrete values for waves of cn and dn types in the limit of strong spatial localization. Simulation of perturbed cnoidal-wave propagation revealed suppression of collapse and multiple-wave filamentation on the developed stage of instability. Different instability scenarios are considered in detail.

DOI: 10.1103/PhysRevE.67.066605 PACS number(s): 42.65.Tg, 42.65.Jx, 42.65.Wi

I. INTRODUCTION

The crucial point for the investigation of propagation dynamics of self-trapped light patterns is their stability with respect to perturbations of the input field distributions. Perturbation-induced decay of unstable patterns can lead to a number of interesting phenomena including the formation of a chain of single and dipole-mode solitons that appear due to the breakup of bright soliton stripes in photorefractive crystals [1–3], generation of a set of optical vortex solitons due to the transverse instability of dark-soliton stripes in photorefractive crystals [4,5] and rubidium vapor [6,7], transverse modulational instability in quadratic nonlinear media [8–10], decay of ring-shaped optical vortices with nonzero angular momentum into diverging solitons in rubidium vapor [11], and quadratic crystals [12,13]. An overview of experimental observations of various types of instabilities of self-trapped light beams in photorefractive, saturable, and quadratic media can be found in [14,15].

Among other types of instabilities there is a steady interest in so-called transverse modulational instability that occurs for two-dimensional self-trapped beams that are localized along one space (or time) coordinate and are uniform along other coordinate. Theoretically this type of instability was considered in a number of physical models including models describing single and incoherently coupled solitons in cubic [16–22], saturable [23] photorefractive [1–5,14,24] and quadratic [12,13,15,25,26] media, discrete solitons [27,28], etc. As a rule, self-trapped light beams or pulses that are stable in one dimension, provided usually that some criteria analogous to the Vakhitov-Kolokolov stability criterion are satisfied [29–36], would be modulationally unstable in two or more dimensions. The bandwidth of the modulational instability domain for localized solitons was calculated analytically and numerically in the frames of the elliptic cubic Schrödinger equation [16–19,37–39]. In the case of the hyperbolic cubic Schrödinger equation the problem of the calculation of the upper boundary of the instability domain for localized solitons is rather complicated and has led to a number of contradictory conclusions [20,38–44]. This problem was solved only recently [14,44]. It is well established that in the frames of the model described by the elliptic Schrödinger equation (for instance, this equation governs the propagation of optical radiation when the diffraction in two transverse directions is taken into account) development of modulational instability leads to wave collapse, whereas in the hyperbolic case (diffraction in one space dimension + normal group velocity dispersion) multiple-wave filamentation occurs in the developed instability regime [45–47].

One of the important problems opened so far is the transverse modulational instability of periodic light patterns or *cnoidal waves*. The properties of these waves are described in Refs. [48–50]. Such waves can serve as a model of periodic arrays of slit laser beams [51–53], trains of optical pulses in fibers [54,55], and electron wave functions in trapped Bose-Einstein condensates [56–58]. In comparison with localized solitons cnoidal waves are described by an additional parameter (so-called *localization degree m*, which is directly related to the wave amplitude and period) and contain localized bright and dark solitons [59] as a limiting case at $m=1$ and delocalized plane waves (for waves of dn type) or low-amplitude harmonic waves (for waves of cn or sn type) at $m=0$.

The transverse modulational instability of cnoidal waves in the frames of the elliptic cubic Schrödinger equation was recently investigated in details in Refs. [60–62]. However, the transverse modulational instability of periodic waves in the frames of the hyperbolic Schrödinger equation was considered earlier only in the context of deep-water gravity waves for one particular case of dn-type waves [43,63]. Moreover, the class of perturbations considered in [43,63] for dn waves was actually very narrow because an assumption about equal periods of perturbation and stationary waves was made. As will be shown in this paper, with this assumption it is impossible to make a conclusion about the true width of the band of modulational instability for periodic waves for both moderate and high (soliton limit) localization degrees. Also, we investigate the transverse modulational instability of spatiotemporal cnoidal waves of cn and sn types, build the whole band of possible growth rates for different

degrees of waves localization, and investigate perturbation-induced transformations of the cnoidal wave patterns on the developed stage of instability.

II. THEORETICAL MODEL AND METHOD OF STABILITY ANALYSIS FOR PERIODIC WAVE PATTERNS

The propagation of laser beams that undergo one-dimensional (1D) diffraction and dispersion in cubic nonlinear medium is described by the dimensionless nonlinear Schrödinger equation for the complex field amplitude $q(\eta,\zeta,\xi)$:

$$i\frac{\partial q}{\partial \xi}=-\frac{1}{2}\frac{\partial^2 q}{\partial \eta^2}+\frac{d}{2}\frac{\partial^2 q}{\partial \zeta^2}+\sigma|q|^2 q. \tag{1}$$

Here amplitude $q(\eta,\zeta,\xi)=(L_{\rm dif}/L_{\rm spm})^{1/2}A(\eta,\zeta,\xi)I_0^{-1/2}$, $A(\eta,\zeta,\xi)$ is the slowly varying envelope, I_0 is the input intensity, $\eta=x/r_0$ is transverse coordinate, $\zeta=(t-z/u_{\rm gr})/\tau_0$ is the retarded time, r_0 and τ_0 are the input beam radius and pulse duration, respectively, $u_{\rm gr}=(\partial k/\partial\omega)^{-1}_{\omega=\omega_0}$ is the group velocity, $k_0=k(\omega_0)$ is the wave number, ω_0 is the carrying frequency, $\xi=z/L_{\rm dif}$ is the normalized propagation distance, $L_{\rm dif}=k_0 r_0^2$ is the diffraction length, $L_{\rm spm}=2c/(\omega_0 n_2 I_0)$ is the self-phase modulation length, $n_2=3\pi\omega_0\chi^{(3)}(\omega_0)/[k(\omega_0)c]$ is the nonlinear coefficient which is proportional to the Fourier transform $\chi^{(3)}(\omega_0)$ of the corresponding element of nonlinear susceptibility tensor, $d=\mathrm{sgn}(\beta_2)L_{\rm dif}/L_{\rm dis}$, $L_{\rm dis}=\tau_0^2/|\beta_2|$ is the dispersion length, and $\beta_2=(\partial^2 k/\partial\omega^2)_{\omega=\omega_0}$.

The first and second terms on the right-hand side of Eq. (1) describe the diffraction and dispersion of self-trapped light patterns, whereas the third term accounts for self-focusing ($\sigma=-1$) or self-defocusing ($\sigma=1$) due to the presence of cubic nonlinearity. It is supposed that the wave field remains uniform along the second spatial coordinate. Modulational instability of cnoidal waves within the frame of the elliptic Schrödinger equation ($d=-1$) was considered in Refs. [60], [62]. Here we concentrate on the hyperbolic case and set $d=1$, which corresponds to the regime of normal group velocity dispersion.

We consider the instability of stationary solutions of Eq. (1) that are periodic along the spatial coordinate η and uniform along the temporal coordinate ζ. Such solutions (cnoidal waves) are given by

$$q_{\rm cn}(\eta,\zeta,\xi)=m\chi\,\mathrm{cn}(\chi\eta,m)\exp[i\xi\chi^2(m^2-1/2)],$$
$$q_{\rm dn}(\eta,\zeta,\xi)=\chi\,\mathrm{dn}(\chi\eta,m)\exp[i\xi\chi^2(1-m^2/2)], \tag{2}$$

in the focusing medium ($\sigma=-1$), and by

$$q_{\rm sn}(\eta,\zeta,\xi)=m\chi\,\mathrm{sn}(\chi\eta,m)\exp[-i\xi\chi^2(1+m^2)/2], \tag{3}$$

in the defocusing medium ($\sigma=1$). Here $\mathrm{cn}(\eta,m)$, $\mathrm{dn}(\eta,m)$, and $\mathrm{sn}(\eta,m)$ are the elliptic functions, $0\leqslant m\leqslant 1$ is the Jacobi parameter that describes localization degree of cnoidal wave, and χ is the form factor. Notice that cnoidal waves (2) and (3) can be written in the general form $q(\eta,\zeta,\xi)=w(\eta)\exp(ib\xi)$, where $w(\eta)$ is the real function describing the phase-modulation-free wave profile and b is the propagation constant. Since it is known that the instability bandwidth is always proportional to $\chi^{1/2}$, further we concentrate on the case $\chi=1$.

To investigate the transverse modulational instability of cnoidal waves we use a linearization technique that is applicable at the initial stage of perturbed wave propagation. We then look for solutions of Eq. (1) in the following form:

$$q(\eta,\zeta,\xi)=\{w(\eta)+[U(\eta,\xi)+iV(\eta,\xi)]\times\cos(\Omega\zeta)\}\exp(ib\xi), \tag{4}$$

where the functions $U(\eta,\xi)$ and $V(\eta,\xi)$ describe the real and imaginary parts of a small ($U,V\ll w$) perturbation, and it is supposed that these functions do not depend on the second transverse coordinate ζ: Ω is the modulation frequency along temporal the ζ axis. Substitution of Eq. (4) into Eq. (1), subsequent linearization, and separation of real and imaginary parts result in the following system of linear differential equations:

$$\frac{\partial U}{\partial\xi}=-\mathcal{L}V,$$
$$\frac{\partial V}{\partial\xi}=\mathcal{R}U. \tag{5}$$

Here the operators $\mathcal{L}=(1/2)(\partial^2/\partial\eta^2)-\sigma w^2(\eta)-b+d\Omega^2/2$ and $\mathcal{R}=\mathcal{L}-2\sigma w^2(\eta)$ are self-adjoint and depend on the coordinate η, parameters σ, d, and m, and modulation frequency Ω of the seed perturbation along the ζ axis. Notice that the nonperturbed cnoidal wave intensity profile is included in right-hand side operators like a given potential and seed modulation frequency is included like a parameter.

We look for solutions of Eqs. (5) in the form of a spectral-type integral representation:

$$U(\eta,\xi)=\mathrm{Re}\left[\int C(\delta)u(\eta,\delta)\exp(\delta\xi)d\delta\right],$$
$$V(\eta,\xi)=\mathrm{Re}\left[\int C(\delta)v(\eta,\delta)\exp(\delta\xi)d\delta\right], \tag{6}$$

where δ is the complex increment (its real part, if positive, describes the perturbation growth rate), $C(\delta)$ is an arbitrary complex function, and $u(\eta,\delta)$ and $v(\eta,\delta)$ are complex perturbation amplitudes that depend on the increment value. Integration goes over all possible increments. Upon substitution of expressions (6) into system (5) and equalization of the terms under integrals with the same exponential coefficients $\exp(\delta\xi)$ one gets the system of linear equations

$$\delta u=-\mathcal{L}v,$$
$$\delta v=\mathcal{R}u. \tag{7}$$

Taking into account expressions for the operators $\mathcal{L}$ and $\mathcal{R}$, one can rewrite the system of equations (7) in the matrix form

$$\frac{d\Phi}{d\eta}=\mathcal{B}\Phi, \quad \mathcal{B}=\begin{pmatrix}\mathcal{O} & \mathcal{E}\\ \mathcal{N} & \mathcal{O}\end{pmatrix},$$

$$\mathcal{N}=\begin{pmatrix}2b-d\Omega^2+6\sigma w^2 & 2\delta\\ -2\delta & 2b-d\Omega^2+2\sigma w^2\end{pmatrix}, \qquad (8)$$

where $\Phi=\{u,v,du/d\eta,dv/d\eta\}^T$ is the solution vector, $\mathcal{O}$ is the 2×2 zero matrix, $\mathcal{E}$ is the 2×2 unity matrix, and the matrix $\mathcal{N}$ depends on the coordinate η, increment δ, parameters σ, d, and m, and modulation frequency Ω. A general solution of Eq. (8) can be written in the form

$$\Phi(\eta)=\mathcal{J}(\eta,\eta')\Phi(\eta'), \qquad (9)$$

where $\mathcal{J}(\eta,\eta')$ is the 4×4 Cauchy matrix, which can be found as a solution of the initial value problem $\partial\mathcal{J}(\eta,\eta')/\partial\eta=\mathcal{B}(\eta)\mathcal{J}(\eta,\eta')$, $\mathcal{J}(\eta',\eta')=\mathcal{E}$, where the coordinate η' serves as a parameter. The matrix of the ''translation'' of the perturbation vector Φ on one wave period T is defined by

$$\mathcal{P}(\eta)=\mathcal{J}(\eta+T,\eta). \qquad (10)$$

It was shown by us in Refs. [61], [62] that a conclusion about stability or instability of the corresponding cnoidal wave can be made on the basis of the consideration of four complex eigenvalues λ_n of the matrix of translation (10). These eigenvalues can be expressed through the traces of matrices $\mathcal{P}$ and $\mathcal{P}^2$. Notice that two of these eigenvalues (say, λ_3 and λ_4) can be omitted since $\lambda_3=1/\lambda_1$ and $\lambda_4=1/\lambda_2$, whereas the components of the corresponding eigenvectors are connected through the following symmetry relations: $u_n(\eta)=u_{n+2}(-\eta)$ and $v_n(\eta)=v_{n+2}(-\eta)$, $n=1,2$. It was shown [61,62] that the perturbation eigenvector $\Phi_n(\eta)$, corresponding to the chosen increment δ, would be limited along the η axis only in the case when the corresponding eigenvalue satisfies the condition $|\lambda_n|=1$. Namely, this condition permits one to select ''allowed'' values of the complex increment. As will be shown later in the case of periodic cnoidal waves with $m<1$, conditions $|\lambda_n|=1$ could be satisfied for the band of increments in contradistinction to the case of localized solitons [14]. Notice that in contradistinction to Refs. [43], [63], we do not require here the components $u(\eta,\delta)$ and $v(\eta,\delta)$ of the perturbation vector to be periodic functions of the coordinate η with period equal to the period T of the stationary cnoidal wave $w(\eta)$. Instead, the period of components u, v constituting a limited perturbation eigenvector can take arbitrary high and low values. It is obvious that the class of perturbations considered here is much wider than that considered in Refs. [43], [63].

Taking into account the relations between pairs of eigenvalues of the translation matrix one can use as perturbation linear combinations of the eigenvectors $\Phi_n(\eta)$ and $\Phi_{n+2}(\eta)$ $(n=1,2)$ with arbitrary coefficients instead of four original eigenvectors. Further we will use symmetric and antisymmetric combinations having the following components:

$$\Sigma_1=(\Phi_1+\Phi_3)/2 \quad \begin{cases}s_1=(u_1+u_3)/2,\\ s_2=(v_1+v_3)/2,\end{cases}$$

$$\Sigma_2=(\Phi_2+\Phi_4)/2 \quad \begin{cases}s_3=(u_2+u_4)/2,\\ s_4=(v_2+v_4)/2,\end{cases}$$

$$A_1=i(\Phi_1-\Phi_3)/2 \quad \begin{cases}a_1=i(u_1-u_3)/2,\\ a_2=i(v_1-v_3)/2,\end{cases}$$

$$A_2=i(\Phi_2-\Phi_4)/2 \quad \begin{cases}a_3=i(u_2-u_4)/2,\\ a_4=i(v_2-v_4)/2.\end{cases} \qquad (11)$$

Notice that for chosen coefficients in Eqs. (11), either real or imaginary part of components s_n and a_n will be zero for purely real or imaginary increments δ. Perturbations, constructed in such a way, do not possess a nontrivial phase modulation along the η axis, whereas the components u_n and v_n have such a modulation and, therefore, travel along the cnoidal wave in the propagation process.

Further upon analysis of the modulational instability of spatiotemporal cnoidal waves we change the modulation frequency Ω, increment δ, and localization parameter m, consider the evolution of eigenvalues $\lambda_{1,2}$, and build areas of the existence of allowed perturbations where $|\lambda_{1,2}|=1$. Since the increment δ is supposed to be a complex number, we fixed $|\delta|$ and scanned $\arg(\delta)$ with a fine step (typically $\sim2\pi/1000$). Then the scanning procedure was repeated for a slightly increased value of $|\delta|$ (step ~0.001); the segment of $|\delta|$ scanning was [0,100]. For purely real or imaginary increments $|\lambda_n(\delta)|$ may be equal to unity in the points where $\arg(\delta)=0$ or $\arg(\delta)=\pi/2$, correspondingly. To find the point in which $|\lambda_n(\delta)|$ goes to unity in the case of complex increments δ we arranged a one-dimensional search along the $\arg(\delta)$ axis. In all practical cases the dependence $|\lambda_n(\delta)|$ on $\arg(\delta)$ has a single well-defined maximum, corresponding to the condition $|\lambda_n|=1$.

III. RESULTS AND DISCUSSION

A. Transverse modulational instability of cn waves

We start with an analysis of the transverse modulational instability of cn waves that was not previously considered in the literature except for the case of $m=1$ (soliton limit). The profile of this wave is described by the first equation of Eqs. (2). First of all, numerical results obtained by us on the basis of the method described in the previous section revealed that in the case of $m=1$, when the cn wave transforms into a single soliton stripe, the modulation instability band is given by $0\leqslant\Omega\leqslant1$, which is consistent with recently reported analytical results [14,44] and is in disagreement with the numerical results of Refs. [38], [40–43], [63], stating that the upper boundary of the modulational instability domain for localized solitons is given by $\Omega\approx1.08$. We have found that for moderate localization degrees $0<m<1$ the modulation frequency band corresponding to perturbations of the cn wave with purely real increments *has no upper limit* in the frames of the hyperbolic cubic Schrödinger equation [Eq. (1)], which is in contradistinction to the case of the elliptic cubic Schrödinger equation [62].

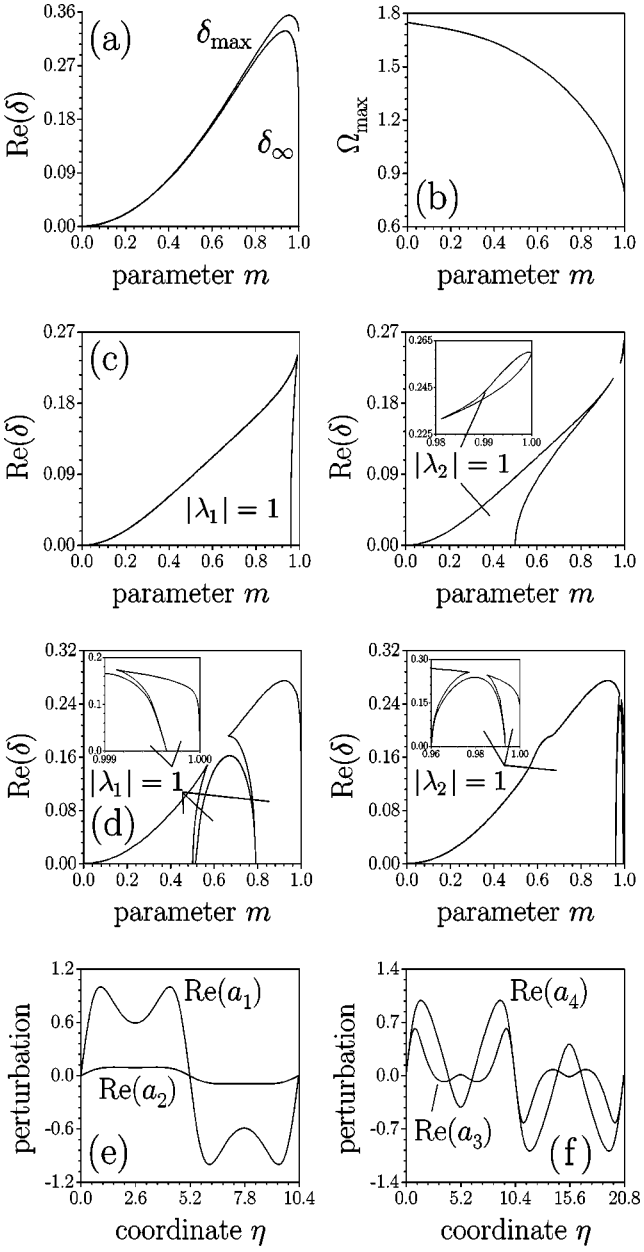

FIG. 1. Dependences of increments δ_{max} and δ_∞ (a) and frequency Ω_{max} (b) on localization parameter m for cn waves. Rows (c) and (d) show the areas of existence of limited perturbations of cn waves corresponding to real increments and modulation frequencies $\Omega=0.5$ and $\Omega=1.5$, respectively. (e) Perturbation profile corresponding to $m=0.95$, $\Omega=0.1$, and $\delta=0.04934$. (f) Perturbation profile corresponding to $m=0.95$, $\Omega=1$, and $\delta=0.20006$.

For a given modulation frequency and parameter $m<1$ one has a *band of possible increments* lying between zero and a certain maximal value. This situation is qualitatively different from the situation for localized solitons when one has a *discrete* spectrum of possible increments [14,44]. For fixed m there always exists an absolute maximum of the increment δ_{max} that is reached for perturbations with a limited modulation frequency Ω_{max}. The dependences of δ_{max} and Ω_{max} on the localization degree m are shown in Figs. 1(a) and 1(b), correspondingly. Notice that δ_{max} goes to zero as $m\to 0$, which is an indication of the obvious fact that instability is suppressed with the decrease of the amplitude of the cn wave. The increment δ_{max} reaches its maximal value at $m\approx 0.96$. The interesting result is that for $\Omega\to\infty$ the upper limit of "allowed" increments δ_∞ exists. This quantity is shown in Fig. 1(a) as a function of the wave localization degree, and one can see that $\delta_\infty\to 0$ as $m\to 1$.

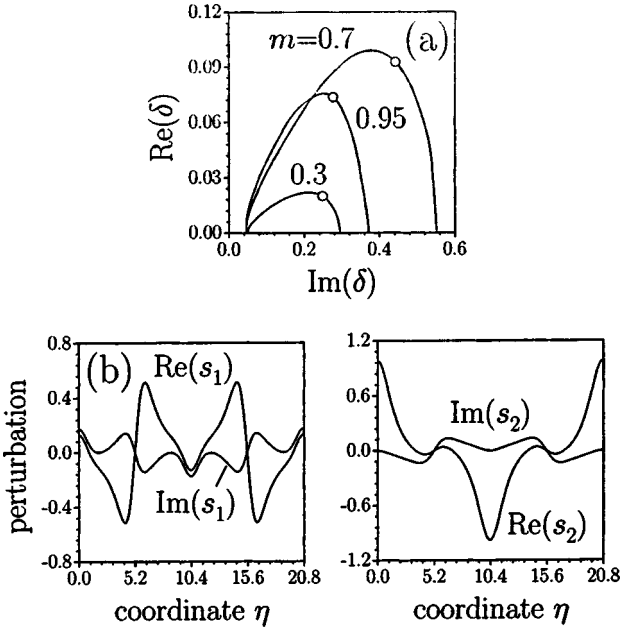

FIG. 2. (a) Curves at the complex plane showing possible increment values for cn waves with various m at $\Omega=0.05$. Condition $|\lambda_1|=1$ is satisfied at the left parts of curves before points marked by circles, whereas $|\lambda_2|=1$ is satisfied at the right parts of the curves. Row (b) shows perturbation profile corresponding to $m=0.95$, $\Omega=0.05$, and $\delta=0.068\,66+0.187\,63i$.

This is direct indication that for $m=1$ (soliton case) the upper limit of the frequency band for exponentially growing perturbations exists, whereas for intermediate m (periodic case) the instability band is unlimited. Notice that the difference between δ_{max} and δ_∞ is rather small in the interval $0<m<0.9$, and perturbations with frequencies from a very wide range can grow with almost equal rates. Such a situation could lead to multiple filamentation of perturbed cnoidal waves or the development of optical turbulence, which is common phenomena in the physical systems driven by hyperbolic Schrödinger equations.

The areas of existence of growing perturbations (areas where one of the conditions $|\lambda_{1,2}|=1$ is satisfied) are shown in rows (c) and (d) of Fig. 1 for $\Omega=0.5$ and 1.5 on the plane (δ,m). For low and high modulation frequencies the areas of existence of growing perturbations contract as $m\to 0$. For high frequencies $\Omega>1$ these areas also vanish as $m\to 1$ [Fig. 1(d)], whereas at low frequencies $\Omega<1$ only the single perturbation with the highest increment exists in the soliton limit $m=1$ [Fig. 1(c)].

Profiles of the perturbations corresponding to different modulation frequencies are shown in Figs. 1(e) and 1(f). For convenience, we normalized the perturbation amplitude to unity. Notice that the perturbations shown are clearly anti-

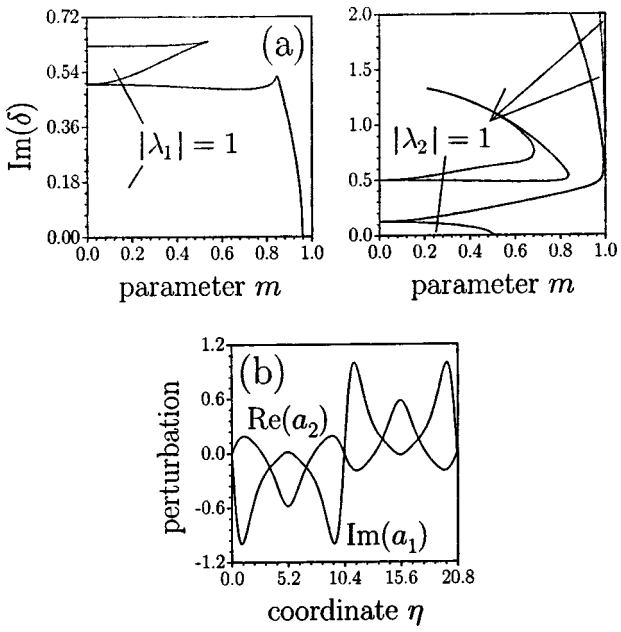

FIG. 3. Row (a) shows areas of existence of limited perturbations of cn waves corresponding to imaginary increments at $\Omega = 0.5$. (b) Profile of the perturbation corresponding to $m = 0.95$, $\Omega = 0.25$, and $\delta = 0.1468i$.

symmetric whereas the profile of stationary cn waves is symmetric. The latter fact indicates the possibility of the development of a snake instability of cn waves.

Besides for the perturbations corresponding to purely real increments, there exist perturbations of cn waves with complex increments $\mathrm{Re}(\delta)\mathrm{Im}(\delta) \neq 0$; thus, oscillatory instabilities are possible for cn waves. Such perturbations were found only for modulation frequencies $\Omega < 1$. All complex increments lie on the certain curve at the complex plane [Re(δ),Im(δ)]. Figure 2(a) shows such curves for cn waves with various localization degrees. Notice that the left parts of these curves correspond to the first eigenvalue of the translation matrix $|\lambda_1| = 1$, whereas the right parts correspond to the second eigenvalue $|\lambda_2| = 1$. As a rule, real parts of increments corresponding to oscillatory instabilities are small compared with their imaginary parts. For complex increments both real and imaginary parts of the components of symmetric and antisymmetric combinations, Eqs. (11), of perturbation eigenvectors are nonzero [Fig. 2, row (b)].

In the case of purely imaginary increments one gets a restricted area of existence of cn wave perturbations corresponding to the eigenvalue λ_1 and an unrestricted area for the eigenvalue λ_2 [Fig. 3, row (a)]. The structure of the latter area becomes more and more complicated with an increase of the modulation frequency and localization degree. A typical profile of the perturbation corresponding to imaginary increments is shown in Fig. 3(b).

To check the results of the linear stability analysis we have solved nonlinear Schrödinger equation (1) numerically by the split-step Fourier method with the input conditions (4). We used an initial perturbation amplitude $\delta q_0 = 0.01$ and followed the dynamics of the perturbed wave. Further, to show the rate of perturbation growth we plot the quantity

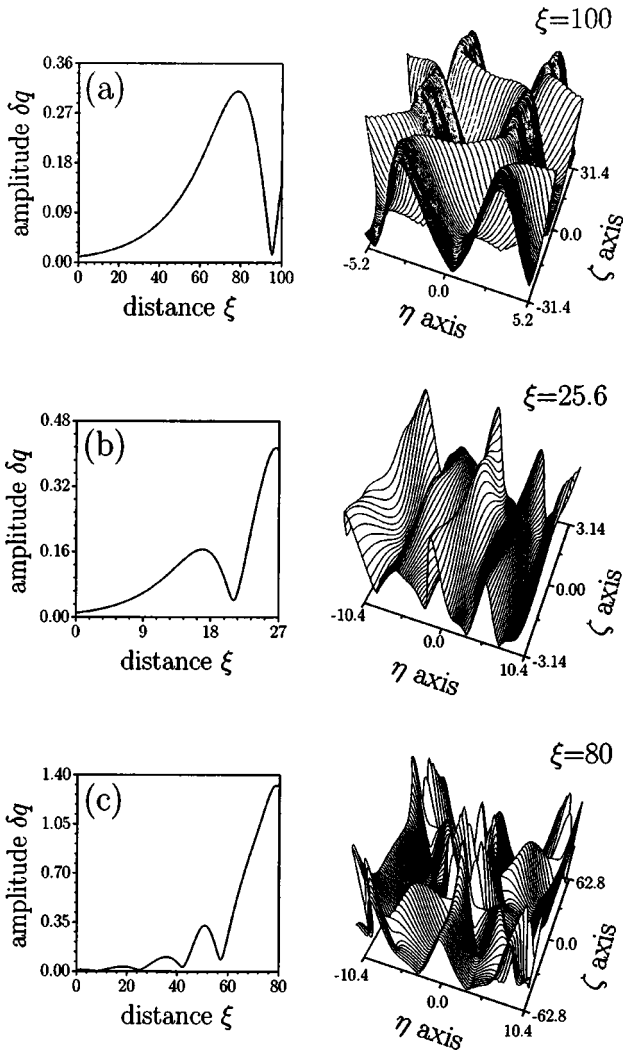

FIG. 4. Rows (a), (b), and (c) show the dependences of the amplitude of perturbations depicted in Figs. 1(e), 1(f), and 2(b), correspondingly, on the propagation distance and final distributions of the field of perturbed cn waves.

$\delta q = |q_p(0,0,\xi)| - |q_s(0,0,\xi)|$ (perturbation amplitude) as a function of propagation distance ξ, where $q_p(\eta,\zeta,\xi)$ is the complex field distribution of perturbed waves and $q_s(\eta,\zeta,\xi)$ is the field distribution of stationary cnoidal waves.

At the initial stage of propagation, the perturbation grows exponentially with distance, according to expression (4). Figure 4(a) shows the dependence of the perturbation amplitude on ξ and final distribution of the field of cn waves in the case of a perturbation with low modulation frequency $\Omega = 0.1$. The development of a snake instability is clearly observed. With the increase of the modulation frequency the snake instability is replaced by the neck one [see Fig. 4, row (b)] finally leading to multiple filamentation of the perturbed cn wave. The development of an oscillatory instability of cn waves is shown in row (c) of Fig. 4.

B. Transverse modulational instability of dn waves

In this section we consider the transverse modulational instability of dn waves that was for the first time analyzed in

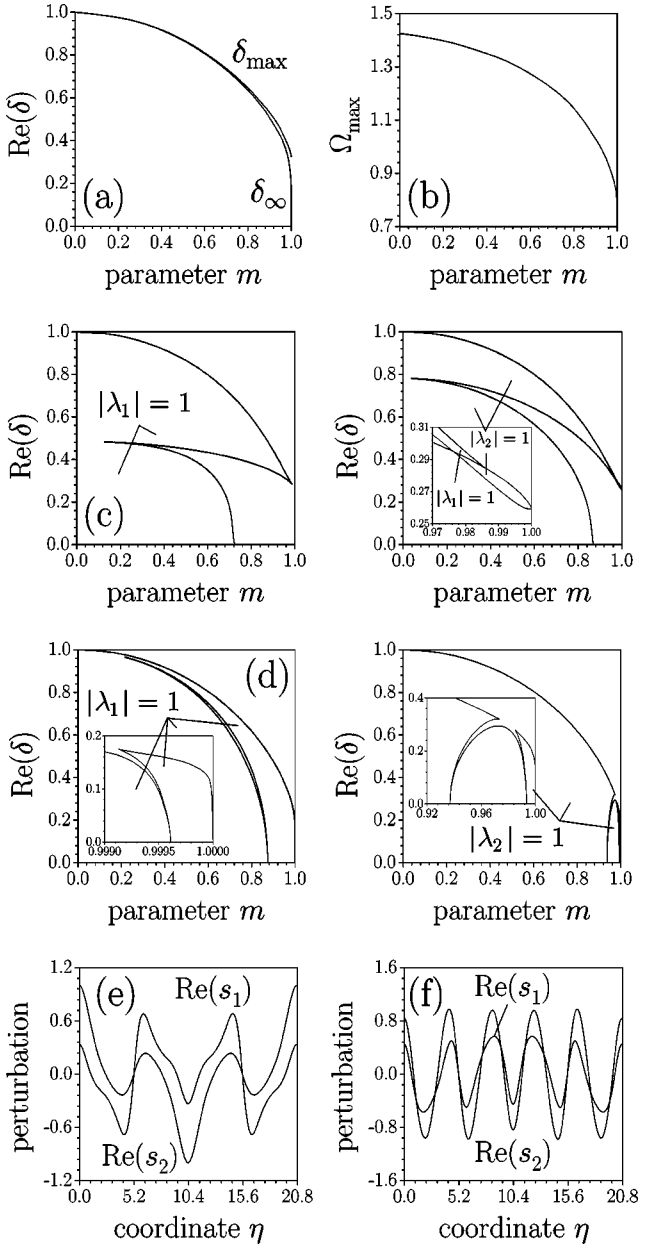

FIG. 5. Dependences of the increments $\delta_{\max}$ and δ_{∞} (a) and frequency $\Omega_{\max}$ (b) on the localization parameter m for dn waves. Rows (c) and (d) show the areas of existence of limited perturbations of dn waves corresponding to real increments and modulation frequencies $\Omega=0.5$ and $\Omega=1.5$, respectively. (e) Perturbation profile corresponding to $m=0.95$, $\Omega=0.1$, and $\delta=0.29679$. (f) Perturbation profile corresponding to $m=0.95$, $\Omega=1.5$, and $\delta=0.316\,01$.

Refs. [43], [63]. We start from purely real increments. With the aid of our method we have found that as in the case of cn waves in the case of dn waves with $m<1$ there is *no upper limit* for the modulation instability domain in contradiction to results of Refs. [43], [63]: i.e., exponentially growing perturbations can still be found as $\Omega\to\infty$. For dn waves there also exists an absolute maximum of the increment $\delta_{\max}$ at frequency $\Omega_{\max}$ and the upper boundary δ_{∞} of the band of "allowed" increments does not depend on Ω as $\Omega\to\infty$ [Figs.

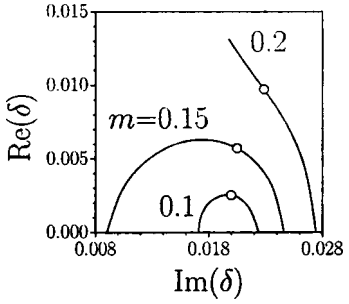

FIG. 6. Curves at the complex plane showing possible increment values for dn waves with various m at $\Omega=0.02$. Condition $|\lambda_1|=1$ is satisfied at the left parts of curves before points marked by circles, whereas $|\lambda_2|=1$ is satisfied at the right parts of the curves.

5(a) and 5(b)]. Notice that analogously to the case of cn waves $\delta_{\infty}\to 0$ as $m\to 1$, whereas $\delta_{\max}$ monotonically decreases to a certain nonzero value. This is a consequence of the fact that for strong spatial localization both cn and dn waves transform into arrays of bright solitons which are in phase for dn waves and out of phase for cn waves. Therefore the modulation frequency band is restricted for $m=1$—i.e., instability is possible for modulation frequencies $0\leqslant\Omega\leqslant 1$—and unrestricted for intermediate localization degrees. The increments $\delta_{\max}$ and δ_{∞} reach their maximal unity value at $m\to 0$, when the dn wave transforms into a plane wave. The modulation frequency $\Omega_{\max}$ corresponding to the maximal increment monotonically decreases with an increase of the localization degree. Since $\delta_{\max}$ and δ_{∞} only slightly differ in the range $0<m<0.9$, multiple filamentation of perturbed dn waves should develop analogously to the case of cn waves.

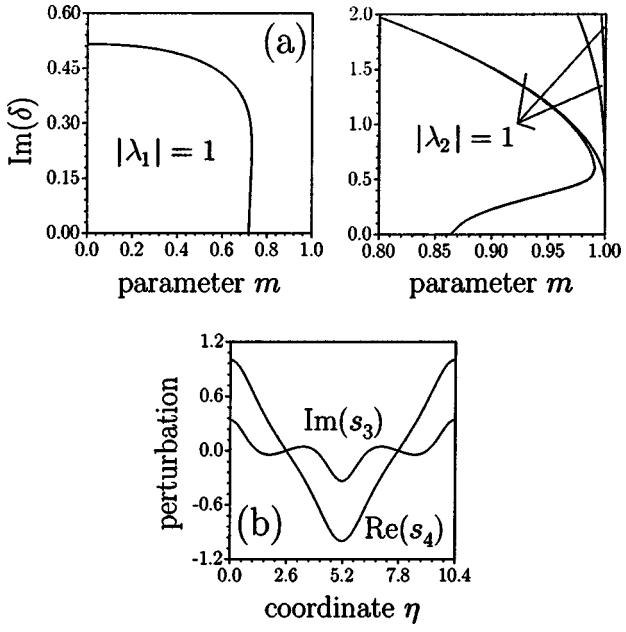

FIG. 7. Row (a) shows areas of existence of limited perturbations of dn waves corresponding to imaginary increments at $\Omega=0.5$. (b) Profile of the perturbation corresponding to $m=0.95$, $\Omega=0.5$, and $\delta=0.375\,84i$.

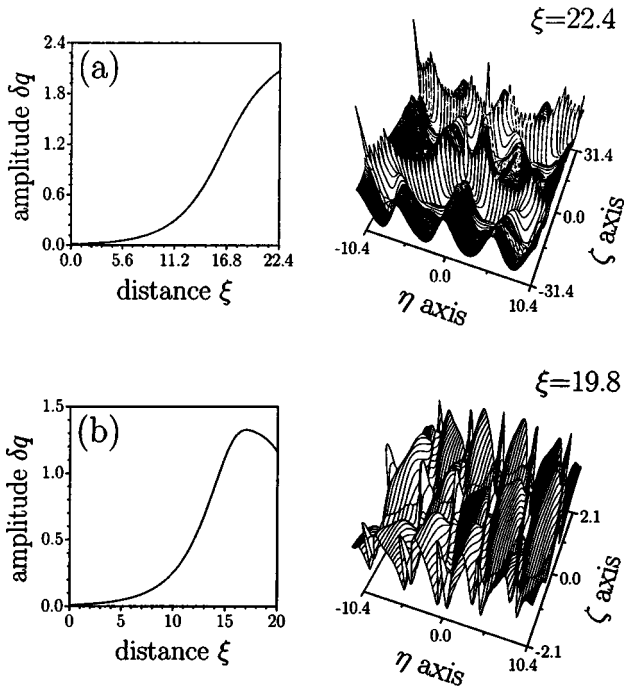

FIG. 8. Rows (a) and (b) show the dependences of the amplitude of perturbations depicted in Figs. 5(e) and 5(f), correspondingly, on the propagation distance and final distributions of the field of perturbed dn waves.

The areas of existence of allowed perturbations of dn waves at the plane (δ,m) for $\Omega=0.5$ and 1.5 are shown in rows (c) and (d) of Fig. 5. One can see that for $\Omega>1$ the areas of existence vanish at $m=1$, whereas for $\Omega<1$ one gets at $m=1$ the only possible increment and single perturbation eigenvector. Notice that the existence of an upper frequency boundary of the instability domain found in Refs. [43], [63] can be easily explained if one takes into account that the requirement of equal periods of perturbation and stationary cnoidal waves corresponds to the case of real eigenvalues $\lambda_{1,2}=\pm 1$ (see Refs. [61], [62] for details). The conditions $\lambda_{1,2}=\pm 1$ are satisfied only for a limited number of curves lying within the area with $|\lambda_{1,2}|=1$ at the (δ,m) plane. Thus imposing requirements of equal periods of perturbation and stationary waves one gets a discrete spectrum of possible increments for cnoidal waves with $m<1$, which is not the case as was shown above. With an increase of the modulation frequency Ω at fixed m values of the increments δ corresponding to the conditions $\lambda_{1,2}=\pm 1$ decreases, and for high enough Ω it is impossible to find exponentially growing perturbations with period equal to the period of cnoidal dn waves. However, there are still exist exponentially growing perturbations with periods *exceeding* the period of cnoidal waves. Numerical integration revealed that periods of growing perturbations corresponding to $\Omega\gg 1$ considerably exceed periods of corresponding cnoidal waves with $m<1$.

Typical perturbation profiles for dn waves corresponding to real increments and two different modulation frequencies $\Omega=0.1$ and $\Omega=1.5$ are shown in Figs. 5(e) and 5(f). Notice that perturbations are symmetric as well as the dn wave itself. Two characteristic scales are clearly seen in the perturbation profiles: the first of them is given by the perturbation period, whereas the second is defined by the period of dn waves.

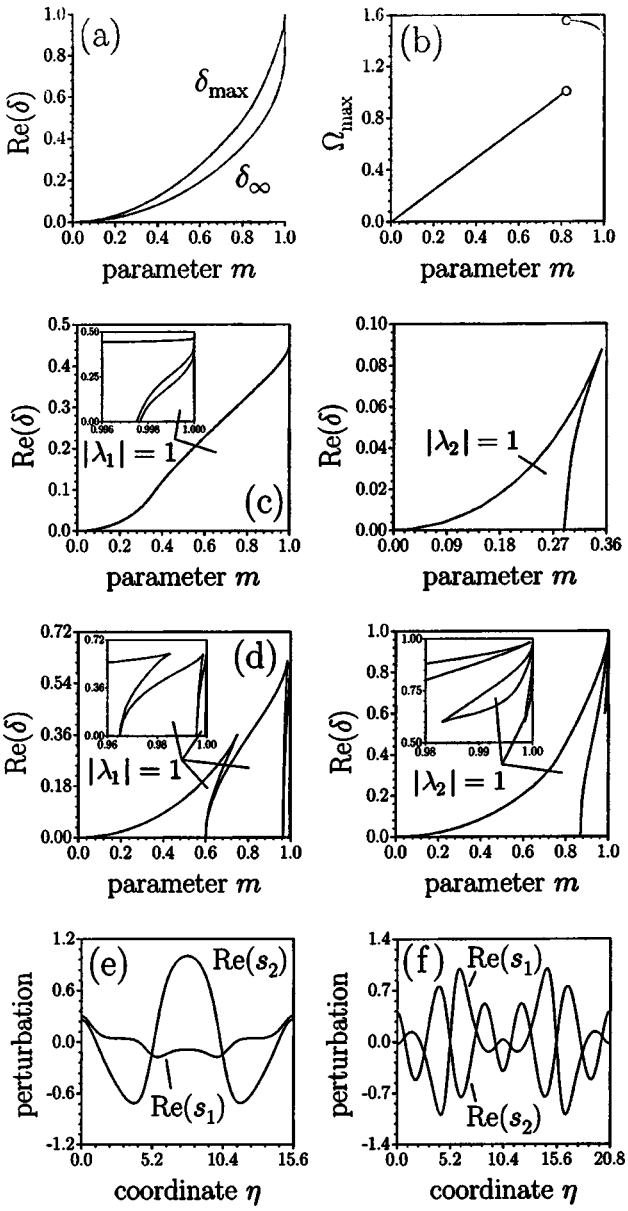

FIG. 9. Dependences of the increments $\delta_{\max}$ and δ_∞ (a) and frequency $\Omega_{\max}$ (b) on the localization parameter m for sn waves. Rows (c) and (d) show the areas of existence of limited perturbations of sn waves corresponding to real increments and modulation frequencies $\Omega=0.5$ and $\Omega=1.5$, respectively. (e) Perturbation profile corresponding to $m=0.95$, $\Omega=0.35$, and $\delta=0.12764$. (f) Perturbation profile corresponding to $m=0.95$, $\Omega=1.5$, and $\delta=0.46191$.

In contradistinction to two-dimensional spatial dn waves [62], spatiotemporal dn waves governed by hyperbolic Schrödinger equation (1) are affected by oscillatory instability: i.e., perturbations with complex increments were found for $\Omega<1$. At fixed m and Ω such complex increments also lie on certain curves at the plane $[\mathrm{Re}(\delta),\mathrm{Im}(\delta)]$ (Fig. 6). We do

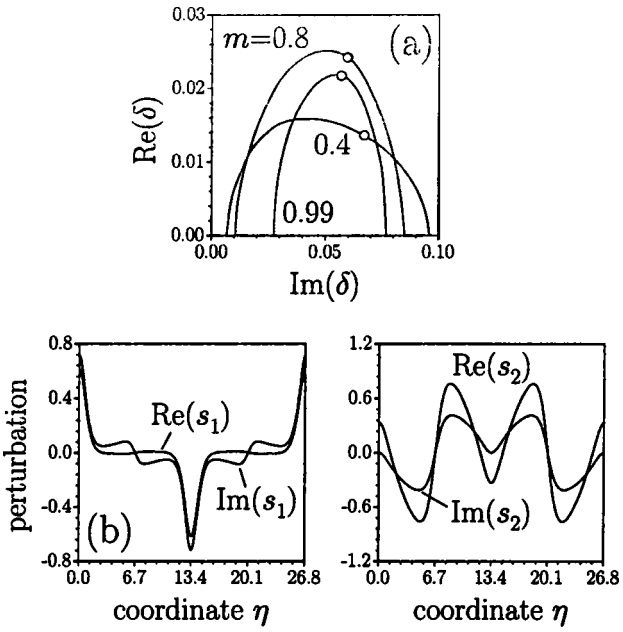

FIG. 10. (a) Curves at the complex plane showing possible increment values for sn waves with various m at $\Omega=0.1$. Condition $|\lambda_1|=1$ is satisfied at the left parts of curves before the points marked by circles, whereas $|\lambda_2|=1$ is satisfied at the right parts of the curves. Row (b) shows the perturbation profile corresponding to $m=0.99$, $\Omega=0.3$, and $\delta=0.055\,45+0.131\,59i$.

not show a typical perturbation profile for this case since periods of such perturbations considerably exceed the period of dn waves, whereas modifications of the perturbation profile occur at the scale given be the period of dn waves.

The areas of existence of allowed perturbations of dn waves with imaginary increments are similar to that for cn

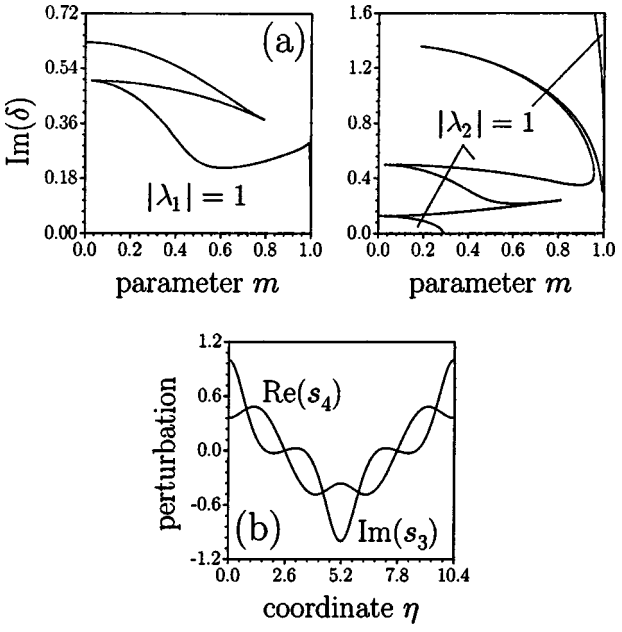

FIG. 11. Row (a) shows the areas of existence of limited perturbations of sn waves corresponding to imaginary increments at $\Omega=0.5$. (b) Profile of the perturbation corresponding to $m=0.95$, $\Omega=1$, and $\delta=0.75181i$.

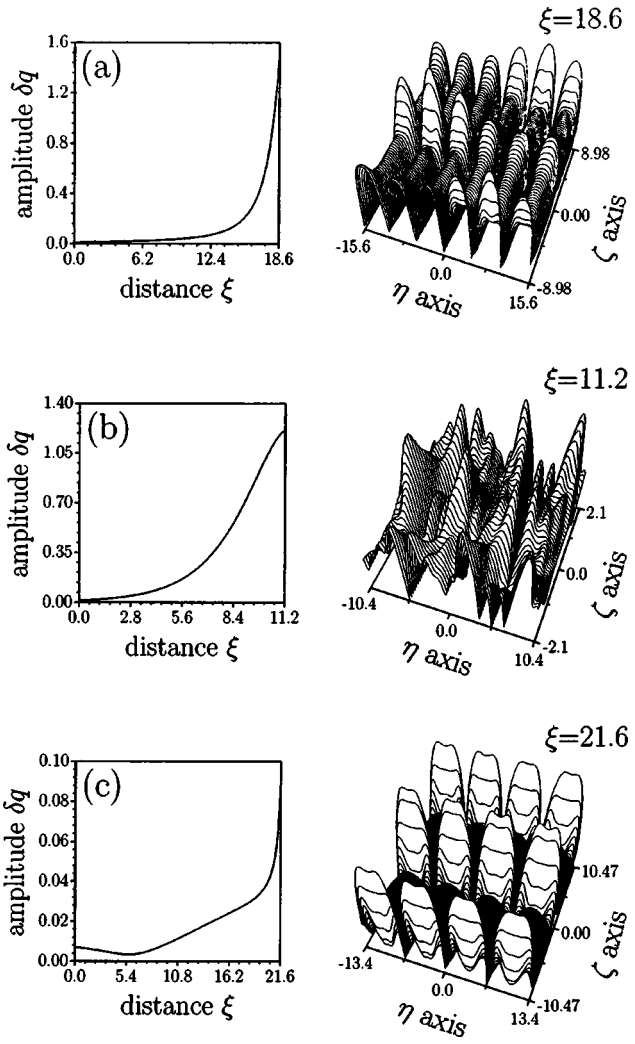

FIG. 12. Rows (a), (b), and (c) show the dependences of the amplitude of perturbations depicted in Figs. 9(e), 9(f), and 10(b), correspondingly, on the propagation distance and final distributions of the field of perturbed sn waves.

waves [row (a) of Fig. 7]. The symmetric perturbation profile corresponding to imaginary increments is shown in row (b) of Fig. 7.

Direct numerical simulation of the propagation of perturbed dn waves confirmed the results of the linear stability analysis. For low modulation frequencies the dynamics of instability development is quite unusual [row (a) of Fig. 8]. It is accompanied by a snakelike distortion of ''odd'' stripes of dn waves, whereas ''even'' stripes remain almost unaffected by instability, except for a considerable increase of the wave amplitude in the rather narrow space regions. For moderate and high modulation frequencies one observes a neck instability, leading to multiple filamentation of dn waves as in the case of cn waves. The initial stage of this process is shown in row (b) of Fig. 8.

C. Transverse modulational instability of sn waves

At the beginning we will consider the case of real increments. For sn waves the maximal increment $\delta_{\max}$ and incre-

ment δ_∞ grow from 0 to 1 with an increase of the localization degree [Fig. 9(a)]. This means that the band of modulation frequencies corresponding to perturbations with real increments remains unrestricted for all degrees of localization. The frequency $\Omega_{\max}$ grows linearly with an increase of m: however, at $m \approx 0.82$ it is possible jump to the higher frequency value that is connected with the complicated multihumped structure of the areas of existence of perturbations at the plane (δ,Ω). There are several jumps of frequency $\Omega_{\max}$, but they are not shown in the chosen scale for the localization degree. The areas of existence of allowed perturbations of sn waves with real increments are shown in rows (c) and (d) of Fig. 9, for frequencies $\Omega = 0.5$ and 1.5, respectively. The width of these areas (at least for eigenvalue λ_1) monotonically increases as $m \to 1$. Typical perturbation profiles for two different modulation frequencies are shown in Figs. 9(e) and 9(f).

We also found perturbations of sn waves corresponding to complex increments [Fig. 10(a)]. The profile of perturbation corresponding to complex increments is shown in row (b) of Fig. 10. Finally, the areas of existence of perturbations with imaginary increments have the same qualitative form as the areas for cn and dn waves (Fig. 11).

Numerical simulation of the propagation of perturbed sn waves revealed a rather unusual regime of instability development for small modulation frequencies [rows (a) and (c) of Fig. 11]. Instability leads to a considerable rise of the field of sn waves in the rather narrow areas corresponding to local maxima or minima of the modulation function $\cos(\Omega\zeta)$ from expression (4). At the same time the remaining part of the sn wave remains almost unchanged upon propagation. Notice that for sn waves we found only scenarios corresponding to neck-type instability. At moderate and high modulation frequencies multiple filamentation of sn waves was usually observed [Fig. 12(b)].

IV. CONCLUSION

In conclusion, we applied a method of analysis of the stability of periodic light patterns, developed in [61,62], to an investigation of the transverse modulational instability of spatiotemporal cnoidal waves in the framework of the hyperbolic nonlinear Schrödinger equation. The areas of existence of allowed perturbations of cnoidal waves of cn, dn, and sn types at the plane increment degree of cnoidal wave localization were found. It was shown that the band of modulation frequencies corresponding to exponentially growing perturbations is restricted only in the self-focusing medium in the bright soliton limit, but it remains unrestricted for sn waves in the defocusing medium in the dark-soliton limit. The development of instability leads as a rule to multiple filamentation of spatiotemporal cnoidal waves.

ACKNOWLEDGMENTS

The authors acknowledge financial support from RFBR under Grant No. 03-02-16370 and from CONACYT under Grant No. 34684-E. The work of Yaroslav V. Kartashov was supported by the Generalitat de Catalunya.

[1] A. V. Mamaev, M. Saffman, and A. A. Zozulya, Europhys. Lett. **35**, 25 (1996).
[2] A. S. Desyatnikov, D. Neshev, E. A. Ostrovskaya, Yu. S. Kivshar, G. McKarthy, W. Krolikowski, and B. Luther-Davies, J. Opt. Soc. Am. B **19**, 586 (2002).
[3] M. Ahles, K. Motzek, A. Stepken, F. Kaiser, C. Weilnau, and C. Denz, J. Opt. Soc. Am. B **19**, 557 (2002).
[4] A. V. Mamaev, M. Saffman, and A. A. Zozulya, Phys. Rev. Lett. **76**, 2262 (1996).
[5] A. V. Mamaev, M. Saffman, D. Z. Anderson, and A. A. Zozulya, Phys. Rev. A **54**, 870 (1996).
[6] V. Tikhonenko, J. Christou, B. Luther-Davies, and Yu. S. Kivshar, Opt. Lett. **21**, 1129 (1996).
[7] V. Tikhonenko, Yu. S. Kivshar, V. V. Steblina, and A. A. Zozulya, J. Opt. Soc. Am. B **15**, 79 (1998).
[8] R. A. Fuerst, D.-M. Baboiu, B. Lawrence, W. E. Torruellas, G. I. Stegeman, S. Trillo, and S. Wabnitz, Phys. Rev. Lett. **78**, 2756 (1997).
[9] A. De Rossi, S. Trillo, A. V. Buryak, and Yu. S. Kivshar, Opt. Lett. **22**, 868 (1997).
[10] A. De Rossi, S. Trillo, A. V. Buryak, and Yu. S. Kivshar, Phys. Rev. E **56**, R4959 (1997).
[11] V. Tikhonenko, J. Christou, and B. Luther-Davies, J. Opt. Soc. Am. B **12**, 2046 (1995).
[12] D. V. Petrov, L. Torner, J. Martorell, R. Vilaseca, J. P. Torres, and C. Cojocaru, Opt. Lett. **23**, 1444 (1998).
[13] S. Minardi, G. Molina-Terriza, P. Di Trapani, J. P. Torres, and L. Torner, Opt. Lett. **26**, 1004 (2001).
[14] Yu. S. Kivshar and D. E. Pelinovsky, Phys. Rep. **331**, 117 (2000).
[15] A. V. Buryak, P. Di Trapani, and S. Trillo, Phys. Rep. **370**, 63 (2002).
[16] E. A. Kuznetsov and S. K. Turitsyn, Sov. Phys. JETP **67**, 1583 (1988).
[17] G. S. McDonald, K. S. Syed, and W. J. Firth, Opt. Commun. **95**, 281 (1993).
[18] C. T. Law and G. A. Swartzlander, Opt. Lett. **18**, 586 (1993).
[19] D. E. Pelinovsky, Yu. A. Stepanyants, and Yu. S. Kivshar, Phys. Rev. E **51**, 5016 (1995).
[20] K. Rypdal and J. J. Rasmussen, Phys. Scr. **40**, 192 (1989).
[21] E. Infeld and R. Rowlands, *Nonlinear Waves: Solitons and Chaos* (Cambridge University Press, Cambridge, England, 1990).
[22] D. V. Skryabin and W. J. Firth, Phys. Rev. E **60**, 1019 (1999).
[23] E. M. Wright, B. L. Lawrence, W. Torruellas, and G. Stegeman, Opt. Lett. **20**, 2481 (1995).
[24] E. Infeld and T. Lenkowska-Czerwinska, Phys. Rev. E **55**, 6101 (1997).
[25] D.-M. Baboiu and G. I. Stegeman, Opt. Lett. **23**, 31 (1998).
[26] D. V. Skryabin and W. J. Firth, Phys. Rev. Lett. **81**, 3379 (1998).
[27] A. B. Aceves, C. De Angelis, G. G. Luther, and A. M.

Rubenchik, Opt. Lett. **19**, 1186 (1994).
[28] A. B. Aceves, G. G. Luther, C. De Angelis, A. M. Rubenchik, and S. K. Turitsyn, Phys. Rev. Lett. **75**, 73 (1995).
[29] M. G. Vakhitov and A. A. Kolokolov, Sov. Radiophys. **16**, 783 (1973).
[30] J. M. Soto-Crespo, N. Akhmediev, and A. Ankiewicz, Phys. Rev. E **51**, 3547 (1995).
[31] D. E. Pelinovsky and Y. S. Kivshar, Phys. Rev. E **62**, 8668 (2000).
[32] A. V. Buryak and Y. S. Kivshar, Phys. Rev. Lett. **78**, 3286 (1997).
[33] L. Torner, D. Mihalache, D. Mazilu, and N. N. Akhmediev, Opt. Lett. **20**, 2183 (1995).
[34] I. V. Barashenkov, Phys. Rev. Lett. **77**, 1193 (1996).
[35] I. V. Barashenkov, D. E. Pelinovsky, and V. E. Zemlyanaya, Phys. Rev. Lett. **80**, 5117 (1998).
[36] V. A. Aleshkevich, Y. V. Kartashov, A. A. Egorov, and V. A. Vysloukh, Phys. Rev. E **64**, 056610 (2001).
[37] V. E. Zakharov and A. M. Rubenchik, Sov. Phys. JETP **38**, 494 (1974).
[38] E. A. Kuznetsov, A. M. Rubenchik, and V. E. Zakharov, Phys. Rep. **142**, 103 (1986).
[39] C. Sulem and P.-L. Sulem, *Nonlinear Schrödinger Equation: Self-focusing Instabilities and Wave Collapse* (Springer, Berlin, 1999).
[40] B. I. Cohen, K. M. Watson, and B. J. West, Phys. Fluids **19**, 345 (1976).
[41] N. R. Pereira, A. Sen, and A. Bers, Phys. Fluids **21**, 117 (1978).
[42] P. G. Saffman and H. C. Yuen, Phys. Fluids **21**, 1450 (1978).
[43] H. C. Yuen and B. M. Lake, *Nonlinear Dynamics of Deep-Water Gravity Waves* (Academic, New York, 1982).
[44] D. Pelinovsky, Math. Comput. **55**, 585 (2001).
[45] L. Berge, Phys. Rep. **303**, 259 (1998).
[46] L. Berge and J. J. Rasmussen, Phys. Rev. A **53**, 4476 (1996).
[47] N. A. Zharova, A. G. Litvak, T. A. Petrova, A. M. Sergeev, and A. D. Yunakovskii, JETP Lett. **44**, 13 (1986).
[48] V. M. Petnikova, V. V. Shuvalov, and V. A. Vysloukh, Phys. Rev. E **60**, 1 (1999).
[49] F. T. Hioe, Phys. Rev. Lett. **82**, 1152 (1999).
[50] V. A. Aleshkevich, V. A. Vysloukh, and Y. V. Kartashov, Quantum Electron. **31**, 257 (2001).
[51] V. Aleshkevich, V. Vysloukh, and Y. Kartashov, Opt. Commun. **173**, 277 (2000).
[52] N. Korneev, A. Apolinar-Iribe, V. A. Vysloukh, and M. A. Basurto-Pensado, Opt. Commun. **197**, 209 (2001).
[53] A. Apolinar-Iribe, N. Korneev, V. Vysloukh, and C. M. Gomez-Sarabia, Opt. Lett. **27**, 2088 (2002).
[54] V. Aleshkevich, Y. Kartashov, and V. Vysloukh, J. Opt. Soc. Am. B **18**, 1127 (2001).
[55] V. Aleshkevich, Y. Kartashov, and V. Vysloukh, Opt. Commun. **185**, 305 (2000).
[56] L. D. Carr, J. N. Kutz, and W. P. Reinhardt, Phys. Rev. E **63**, 066604 (2001).
[57] J. C. Bronski, L. D. Carr, R. Carretero-Gonzalez, B. Deconinck, J. N. Kutz, and K. Promislow, Phys. Rev. E **64**, 056615 (2001).
[58] J. C. Bronski, L. D. Carr, B. Deconinck, J. N. Kutz, and K. Promislow, Phys. Rev. E **63**, 036612 (2001).
[59] A. Ankiewicz, W. Krolikowski, and N. N. Akhmediev, Phys. Rev. E **59**, 6079 (1999).
[60] V. P. Kudashev and A. B. Mikhailovsky, Sov. Phys. JETP **63**, 972 (1986).
[61] Ya. V. Kartashov, V. A. Aleshkevich, V. A. Vysloukh, A. A. Egorov, and A. S. Zelenina, Phys. Rev. E **67**, 036613 (2003).
[62] Ya. V. Kartashov, V. A. Aleshkevich, V. A. Vysloukh, A. A. Egorov, and A. S. Zelenina, J. Opt. Soc. Am. B **20**, 1273 (2003).
[63] D. U. Martin, H. C. Yuen, and P. G. Saffman, Wave Motion **2**, 215 (1980).